UPSCALING FROM CORE DATA TO PRODUCTION: CLOSING THE CYCLE. A CASE STUDY IN THE SANTA BARBARA AND PIRITAL FIELDS, EASTERN VENEZUELA BASIN

PORRAS, Juan Carlos, Petróleos de Venezuela S.A.
BARBATO, Roberto, Petróleos de Venezuela S.A.
SALAZAR, Diomedes, Universidad de Oriente

ABSTRACT

The Santa Barbara and Pirital fields are located in the North Monagas trend in the Eastern Venezuela Basin. Reservoirs in this trend are characterized by high initial temperature and pressure, and high initial production rates. A tar mat is present at the base of the oil column, acting as a barrier between the aquifers below and the oil-containing formations above. The drive mechanism is solution gas drive and fluid expansion, with reservoir pressure declining rapidly. The hydrocarbon column varies from a gas-condensate cap at the top of the structure to heavy oil at the bottom.

The petrophysical characterization incorporated the analysis of the complex variations in pore and pore throat size that control initial and residual fluid distribution and fluid flow through the reservoirs. Conventional core porosity and permeability, mercury injection capillary pressure, relative permeability, and mineralogical data were used to characterize the reservoir into rock types having similar flow and storage capacity. Water saturation, all of which is considered immobile, was found to be dependent on rock type, with pore throat being the dominant control on the flow characteristics of the reservoirs. Mercury injection capillary pressure data provided useful information about effective pore throat radii, which were semi-quantitatively related to several reservoir responses, such as permeability, porosity, irreducible water saturation, and a capillary pressure profile or pore throat type curve.

A methodology was developed to estimate flow behavior of the different flow units from the integration of rock, reservoir and fluid properties, analyzing the variables that affect production logs, reservoir conditions and the rock types determined. Production curves per foot of perforated interval, curves representing rock quality and a modification of the Vertical Stratigraphic Flow and Storage Diagram were used to cross-correlate different parameters in order to define relations between production rates and rock types, considering the effect of pressure differential between the borehole and the formation, as well as the characteristics of the fluids present in the formation. A clear relation was obtained between rock properties of the perforated zones and the production that they contribute to the total well influx. As expected, better relations were encountered for oil-producing than for gas/condensate-producing wells, since gas production is less dependent on rock quality.

The determination of rock types from core data and the integration with production data for the definition of zones with similar flow characteristics is fundamental for appropriate reservoir characterization.

INTRODUCTION

The Santa Barbara and Pirital Fields are located in the North Monagas Area, Eastern Venezuela Basin (Fig. 1). The stratigraphic column the area comprises approximately 17000 ft. of Cretaceous to Plio-Pleistocene sediments. The reservoirs of interest are under normal pressure conditions and the main depositional environment is deltaic to shallow marine. The main completion method in the area is perforation through casing.

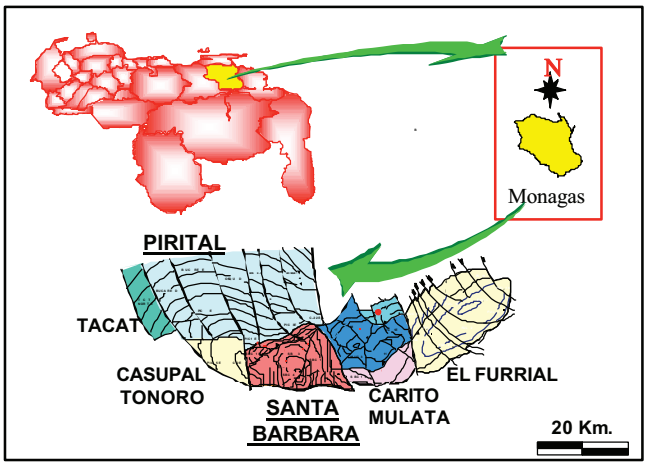

Fig. 1-Relative location map of the Santa Barbara Field, Monagas State, Eastern Venezuela Basin.

The complex pore system present in the area made necessary a detailed petrophysical model based on the study of pore and pore throat size, integrated with sedimentological and production data. Pore throat size may be estimated from routine core porosity and permeability data at ambient conditions. Combining these data with mercury injection capillary pressure results, Winland (1972) developed an empirical relationship between porosity, air permeability and pore aperture corresponding to a mercury saturation of 35% (R35). The Winland equation was published by Kolodzie (1980) and is given below:

$$\text{Log}(R35) = 0.732 + 0.588\text{Log}(k_{air}) - 0.864\text{Log}(\phi) \qquad \textbf{(Eq. 1)}$$

where R35 is the pore aperture radius (microns) corresponding to the 35th percentile, k_{air} is uncorrected air permeability (md), and ϕ is porosity (%). R35 pore throat radius is defined as the pore throat size from mercury injection capillary pressure data where the non-wetting fluid (mercury) saturates 35% of the porosity.

In 1992, Pittman, based on Winland's work, developed R35-type equations for pore throats corresponding to mercury saturations from 10% to 75%. Different techniques were used to determine which of these equations best fitted the study area. Conventional core porosity and permeability data from 17 key wells, and mercury injection capillary pressure data from 11 of these wells, were used to determine the pore throat and the petrophysical model of the area.

The analysis of production data and the correlation with petrophysical parameters was necessary to validate the petrophysical model. This study intended to establish relations between flow rates and the corresponding rock types for the different producing intervals, with the purpose of predicting production rates from petrophysical properties. Production rate depends on variables such as differential pressure and fluid type, making difficult the comparison with discrete petrophysical properties. To simplify this scenario, it was necessary to standardize some of these variables in order to establish tangible relations with petrophysical parameters.

Detailed study of production logs demonstrated that the percentage of flow contributions remained constant regardless of differential pressure. When production log tests are performed and choke sizes are changed, flow rates of the producing intervals vary; however, the percentage of the total rate contributed by each interval remains constant. This allows the study of production logs disregarding the effect of differential pressure, and made possible the correlation between production and petrophysical data.

SEDIMENTOLOGICAL ANALYSIS

Previous studies in the area identified 10 sedimentary facies, mainly based on the variations in grain size and sedimentary structures:

***S*:** Coarse- to very coarse-grained sandstone, sometimes conglomeratic, moderate to poorly sorted, low angle cross stratification, occasionally massive, oil-stained.

***S3*:** Medium- to coarse-grained sandstone, moderate to well sorted, frequent low angle cross stratification, occasionally massive, moderately oil-stained.

***S11*:** Fine- to medium-grained sandstone, moderate to well sorted, generally massive, occasional low angle cross stratification, moderate to highly oil stained, little or absent bioturbation.

***S1*:** Fine- to medium-grained sandstone, well sorted, with continuous dark gray clay laminae, low or absent oil stain, little or absent bioturbation.

***S2*:** Fine- to very fine-grained sandstone, moderate to well sorted, with non-continuous dark gray clay laminae, low or absent oil stain, little or absent bioturbation.

***Sbp*:** Fine- to very fine-grained sandstone, moderate to well sorted, intensely bioturbated, frequent low angle cross stratification, poor or absent oil stain.

***ST*:** Massive light gray siltstone.

***H*:** Dark gray shale, interbedded with well sorted fine-grained sandstone, occasional parallel stratification and ripples, poor or absent oil stain.

***L*:** Dark gray shale.

***C*:** Coal.

PETROPHYSICAL CHARACTERIZATION

The petrophysical characterization incorporated the analysis of the complex variations in pore and pore throat size that control initial and residual fluid distribution and fluid flow through the reservoirs.

Porosity core data at reservoir conditions were available, and used in the core-log correlation. Porosity was calculated from density and neutron logs and calibrated with core data (Fig. 2). Compressibility tests performed on core plugs indicate that confining pressure has a minor effect on porosity.

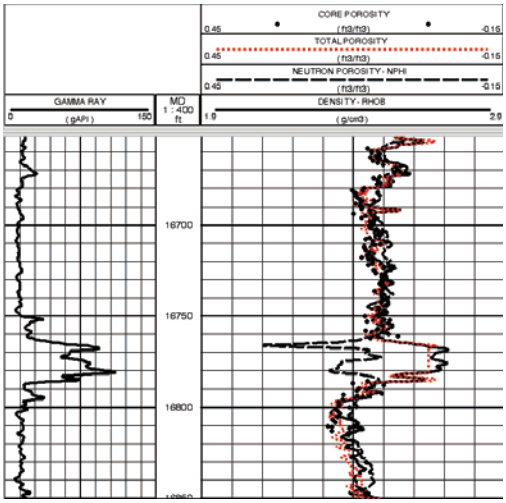

Fig. 2-Plot showing log density (RHOB) and neutron porosity (NPHI), compared to Core Porosity and Calculated Total porosity

In order to determine the most appropriate equation for estimating pore throat size in the study area, plots of pore throat radius from capillary pressure data versus pore throat radius obtained from Pittman's equations were constructed (Fig. 3). As shown in the figure, the R45 equation best honors and reproduces core capillary pressure data, and was therefore selected to estimate pore throat radius in the area. Pitmann's R45 equation is shown below:

$$\text{Log}(R45) = 0.609 + 0.608\text{Log}(k_{air}) - 0.974\text{Log}(\phi) \qquad \textbf{(Eq. 2)}$$

where R45 is the pore aperture radius (microns) corresponding to the 45th percentile, k_{air} is uncorrected air permeability (md), and ϕ is porosity (%). R45 pore throat radius can then be defined as the pore throat size from capillary pressure data where the non-wetting fluid (mercury) saturates 45% of the porosity. Once the equation to be used in the area was determined, R45 pore throat was calculated for both ambient and reservoir conditions.

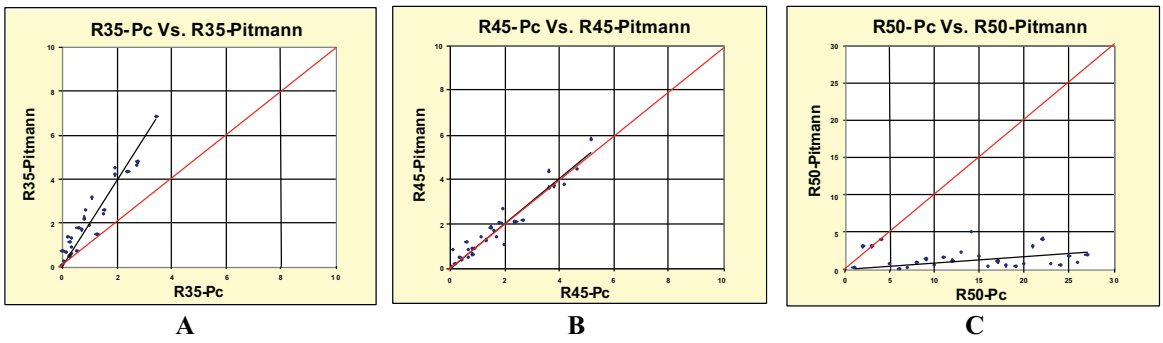

Fig. 3- Pore throat radii estimated from mercury injection capillary pressure data (x-axis) versus calculated pore throat radii (y-axis), showing the best correlation with Pitmann's R45 (Plot B)

The absence of an active aquifer in the area, as well as the extreme length of the hydrocarbon column (>5000 ft.), causing extreme buoyancy pressure, have reduced the residual water saturation in these reservoirs to immobile. Therefore, changes in resistivity and water saturation variations, at a common height in the reservoir, are entirely due to changes in pore geometry. Based on this premise, R45 was plotted against water saturation (Fig. 4), to determine a relationship between both properties. The results shown in figure 4 indicate that water saturation is directly associated to the geometry of the pore system, and can be used in areas where the mobile fluid is hydrocarbon, and the water existent in the formation is considered irreducible. Residual water saturation, as a function of pore type and buoyancy pressure, was obtained from capillary pressure data (Fig. 5).

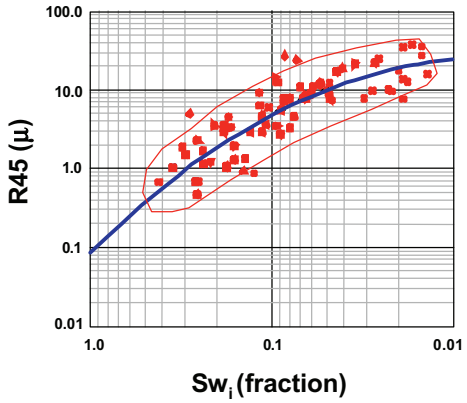

Fig. 4-Pore throat radius (R45) vs. residual water saturatión (Sw$_i$)

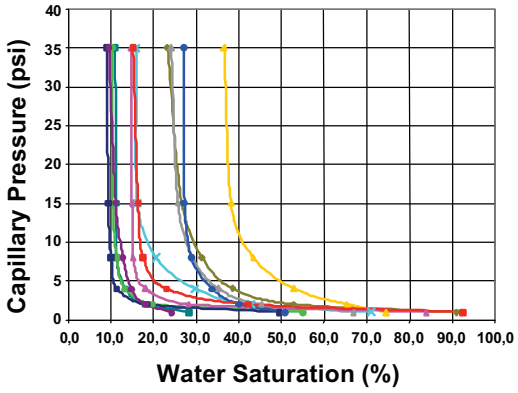

Fig. 5-Air-brine capillary pressure data

Reservoir rock was classified based on R45 pore throat radius, which is the dominant control on the permeability and flow characteristics of the reservoirs. The reservoir rock was divided into five petrophysical categories

Megaporous, defined by a pore throat radius > 10 microns
Macroporous, defined by a pore throat radius between 2.5 and 10 microns
Mesoporous, defined by a pore throat radius between 0.5 and 2.5 microns
Microporous, defined by a pore throat radius between 0.2 and 0.5 microns
Nannoporous, defined by a pore throat radius < 0.2 microns

Mercury injection capillary pressure data (Fig 6) and porosity versus permeability plots (Fig. 7), with superimposed pore throat radii lines obtained using Pittman's R45 equation were used in the recognition of rock types.

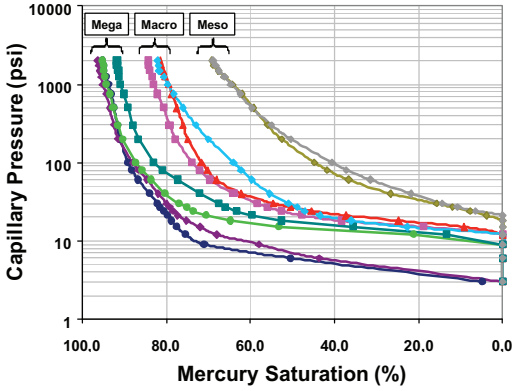

Fig. 6-Mercury injection capillary pressure showing data showing different rock types

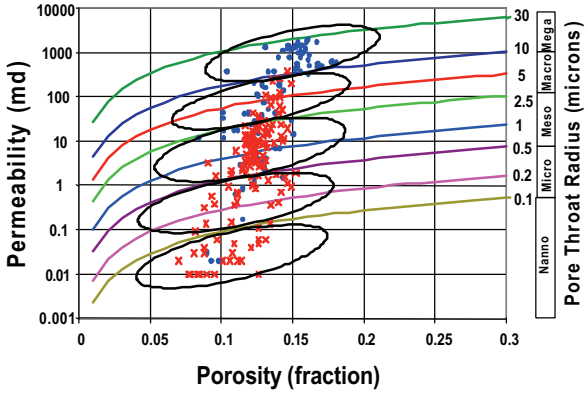

Fig. 7-Porosity versus permeability plot pore throat lines and rock type classification

A rock type curve was then generated for each well. Rock types can be semi-quantitatively related to several reservoir response characteristics useful in formation evaluation, such as permeability to porosity ratio, immobile water saturation, initial production rates, and a capillary pressure profile.

Once porosity was estimated, and R45 pore throat radius was obtained from water saturation, permeability was calculated using Equation 2, and calibrated with core data. Five different equations to estimate permeability were obtained from the porosity versus permeability plots by rock type, at reservoir conditions.

PRODUCTION LOG ANALYSIS

Production logs were normalized to eliminate the effects of differential pressure on flow rates. Flow rates are also dependent on the thickness of the perforated interval, and a methodology to minimize the effect of thickness was also implemented. From the analysis of the flowmeter and assuming a linear relation between revolutions per second (RPS) and fluid velocity at the bottom of the wellbore, the percentage of the total flow rate corresponding to a given interval was estimated as follows:

$$\%Q\,(A) = \{[RPS\,(Top_A) - RPS\,(Base_A)] \,/\, [RPS(100) - RPS\,(0)]\} * 100 \qquad \textbf{(Eq. 3)}$$

where: *%Q (A)* = Percentage of total flow rate for interval A
RPS (Top_A) = RPS measured at top of interval A
RPS ($Base_A$) = RPS measured at base of interval A
RPS (100) = RPS at 100% flow rate
RPS (0) = RPS at 0% flow rate

These intervals correspond not only to isolated sandstones, but also to sections of perforated sandstones that presented variations in the spinner measurements. Therefore, sub-intervals with different production behavior were defined. The following diagram shows the procedure used to determine the percentage contribution of the different producing zones:

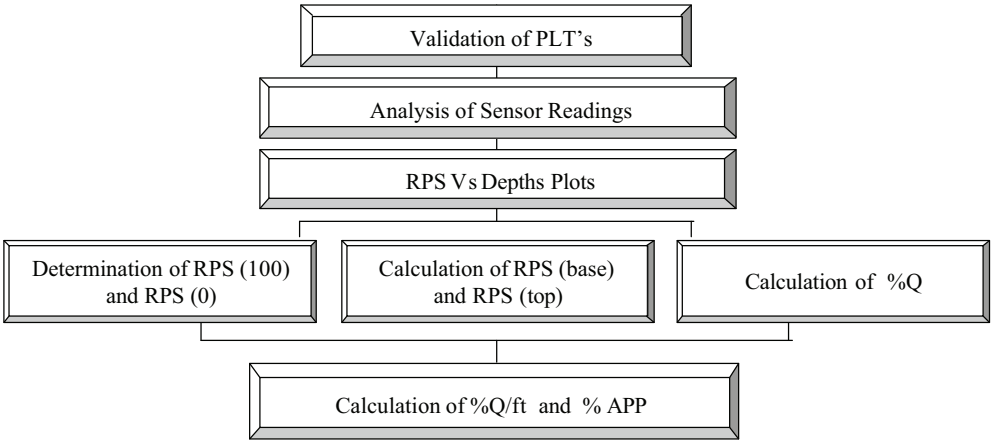

Fig. 8-Flow diagram for analysis of production logs

Thicker intervals present higher percentage of flow contribution when compared to thinner intervals, independently of rock quality. This made necessary the normalization of flow contribution according to interval thickness. A new variable, APP, which is the flow contribution per foot, was then introduced, and calculated as follows:

$$APP = \%Q / H, \qquad \textbf{(Eq. 4)}$$

where: *APP* = Flow contribution per foot, %/ft.
%Q = percentage flow rate, %
H = interval thickness, ft.

APP values and rock type curves were then graphically compared (Fig. 9). In this figure, rock types (PF) are identified with numbers 1 to 9, and APP values (%/ft) depend on the percentage contribution and thickness of the perforated zones. Different graphs were constructed to help locate zones with better conditions for fluid storage and flow: (A) Winland Plots, which show porosity versus permeability data with pore throat lines superimposed; (B) Modified Lorenz Plots, which rank flow units according to their flow capacity (K*H) and storage capacity (Phi*H) expressed in percentage and ordered as a function of decreasing K/Phi ratio; and (C) Stratigraphic

Flow and Storage Profile, which displays, in a stratigraphic or vertical manner, the same information presented in the Modified Lorenz Plot. These graphs are shown in figure 10.

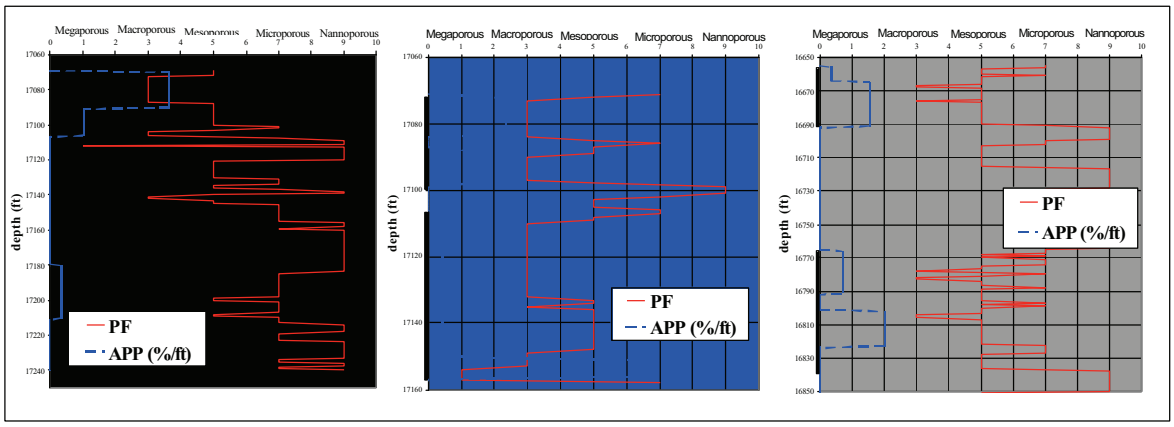

Fig. 9-Comparison between rock type curves (PF) and APP

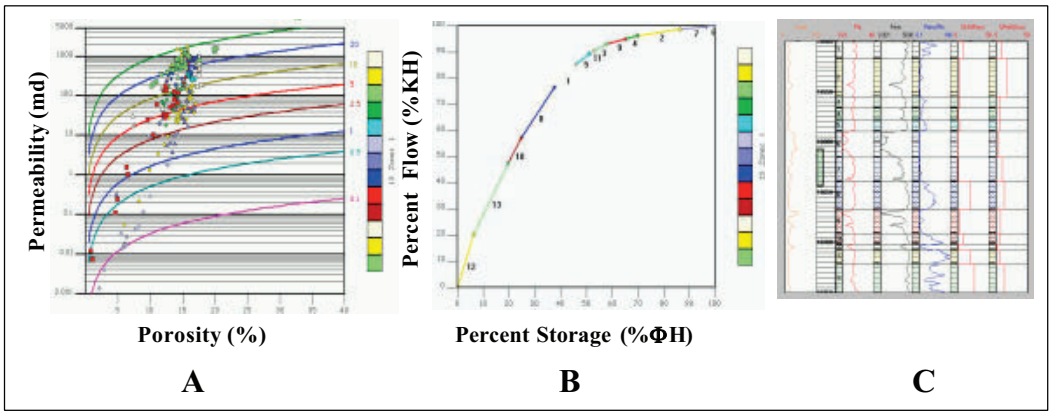

Fig. 10-(A) Winland Plot, (B) Modified Lorenz Plot, (C) Stratigraphic Flow and Storage Profile

The integration of production and petrophysics was made considering the following petrophysical variables each producing interval:

- *% K_i/H_i* = weighted average by rock type, of the permeability of each individual perforated producing interval within a producing zone, expressed in percentage.
- *% $R45_i/H_i$* = weighted average by rock type, of the pore throat radius of each individual perforated producing interval within a producing zone, expressed in percentage.
- *% PHI_i/H_i* = weighted average by rock type, of the porosity of each individual perforated producing interval within a producing zone, expressed in percentage.
- *% $FUSM_i$* = relation between $\%K_i/H_i$ and $\%PHI_i/H_i$ for a given interval, expressed in percentage.

These variables were associated to rock type. For instance, the weighted average of permeability by rock type for each producing interval was calculated as follows:

$$\left(\frac{Ki}{Hi}\right)_j = \left(\frac{K_{mega}}{H_{mega}} + \frac{K_{macro}}{H_{macro}} + \frac{K_{meso}}{H_{meso}} + \frac{K_{micro}}{H_{micro}} + \frac{K_{nanno}}{H_{nanno}}\right)\Bigg]_j \qquad \textbf{(Eq. 5)}$$

In the previous equation, ***j*** represents the producing interval and ***i*** the rock type (mega, macro, meso, micro and nannoporous). Then K_i/H_i for the total producing zone was calculated as follows:

$$\left(\frac{Ki}{Hi}\right)_{total} = \sum_{j=1}^{n}\left[\left(\frac{K_i}{H_i}\right)_j\right] = \left(\frac{K_i}{H_i}\right)_1 + \left(\frac{K_i}{H_i}\right)_2 + \left(\frac{K_i}{H_i}\right)_3 + \ldots\ldots\ldots + \left(\frac{K_i}{H_i}\right)_n \qquad \textbf{(Eq. 6)}$$

where ***j*** represents the producing interval, ***i*** the rock type and ***n*** the number of producing intervals in the producing zone. The percentage of K_i/H_i is then calculated for each interval:

$$\%\left(\frac{Ki}{Hi}\right)_j = \left(\left(\frac{Ki}{Hi}\right)_j \Big/ \left(\frac{Ki}{Hi}\right)_{total}\right) * 100 \qquad \textbf{(Eq. 7)}$$

A similar procedure was used to calculate porosity weighted average (PHI_i/H_i) and pore throat weighted average ($R45_i/H_i$). The relation $FUSM_i = (\%K_i/H_i)/(\%PHI_i/H_i)$, was converted to percentage in the same way as ($\%K_i/H_i$).

DISCUSSION OF RESULTS

In order to correlate the normalized petrophysical variables with production, the production contribution per foot (APP) was also normalized for each interval and converted to percentage, as follows:

$$\%APP_j = APP_j / APP_{total} \qquad \textbf{(Eq. 8)}$$

where: APP_j = flow contribution per foot of interval *j*

APP_{total} = sum of the contribution of the different intervals of the producing zone

The correlation between %APP and the normalized petrophysical variables ($\%K_i/H_i$ and $\%FUSM_i$), is shown in figure 11. Crossplots between all variables involved were constructed considering the type of fluid produced. Figure 12 shows the relation between %APP and %K/H for oil-producing (28-35 °API) and gas/condensate-producing wells (35-41 °API).

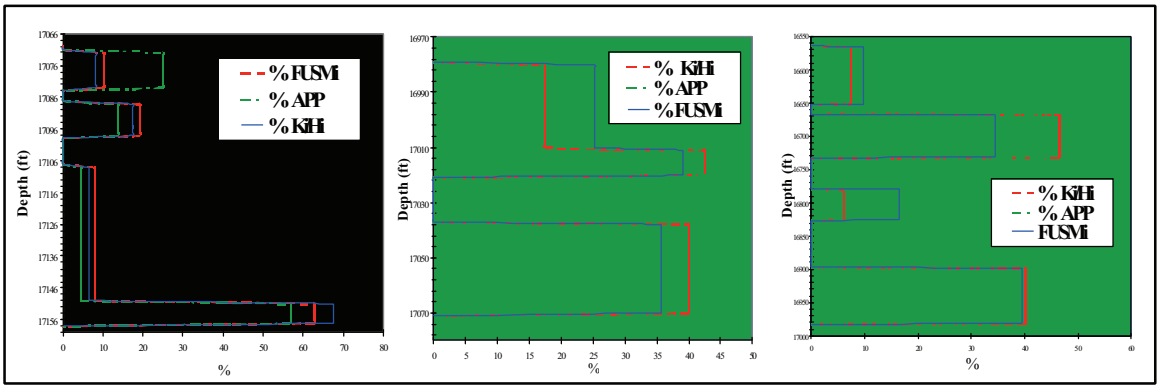

Fig. 11-Comparison between %APP, %Ki/Hi, and %FUSMi

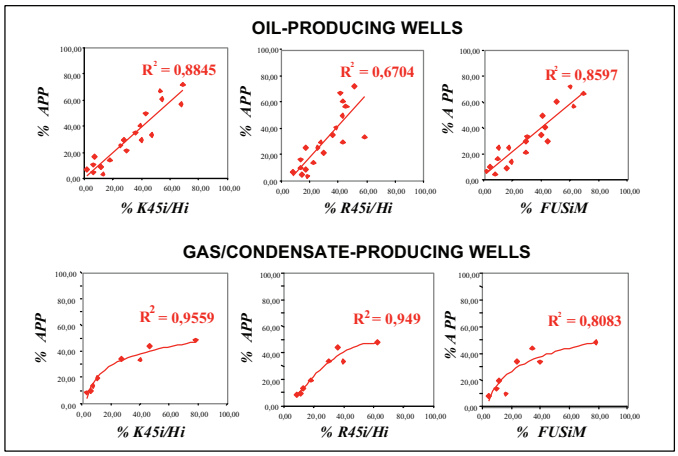

Fig. 12-Relation between %APP and %K/H, for oil- and gas/condensate producing wells

Intervals that presented better storage and flow capacity according to the Modified Lorenz Plots, were also the zones with higher %APP. %APP values do not directly represent the production of a given zone, since they are influenced by the thickness of the producing interval. In order to convert %APP to flow rate (Q), equation systems that consider the number and thickness of producing zones were developed. From equations 4 and 8, the following relations were obtained:

$$\%APP = Qj / Hj * APP_{total} \qquad \textbf{(Eq. 9)}$$

$$\%Q_j = \%APP * H_j * (APP_1 + APP_2 + \ldots + APP_j + \ldots + APP_n) \qquad \textbf{(Eq. 10)}$$

where ***j*** represents a given interval and ***n*** is the number of producing zones. If C_j is defined as:

$$C_j = \%APP_j * H_j \qquad \textbf{(Eq. 11)}$$

Then, re-arranging equation 10:

$$\frac{\%Q_j}{\mathrm{C_j}} = \frac{\%Q_1}{H_1} + \frac{\%Q_2}{H_2} + \ldots + \frac{\%Q_j}{H_j} + \ldots \frac{\%Q_n}{H_n} \qquad \textbf{(Eq. 12)}$$

From equation 12 the system of equations that allow the determination of percentage flow rate (%Q) from percentage flow contribution per foot (%APP) and interval thickness (H), is obtained. For instance, for a well with three producing zones, the system of equations would be:

$$\left(\frac{1}{C_1} - \frac{1}{H_1}\right) * \%Q_1 - \left(\frac{1}{H_2}\right) * \%Q_2 - \left(\frac{1}{H_3}\right) * \%Q_3 = 0 \qquad \textbf{(Eq. 13)}$$

$$-\left(\frac{1}{H_1}\right) * \%Q_1 + \left(\frac{1}{C_2} - \frac{1}{H_2}\right) * \%Q_2 - \left(\frac{1}{H_3}\right) * \%Q_3 = 0 \qquad \textbf{(Eq. 14)}$$

$$-\left(\frac{1}{H_1}\right) * \%Q_1 - \left(\frac{1}{H_2}\right) * \%Q_2 + \left(\frac{1}{C_3} - \frac{1}{H_3}\right) * \%Q_3 = 0 \qquad \textbf{(Eq. 15)}$$

$$\%Q_1 + \%Q_2 + \%Q_3 = 100 \qquad \textbf{(Eq. 16)}$$

In this system the unknowns are %Q1, %Q2, and %Q3. Knowing the %APP and the thickness of the producing intervals, the percentage contributed by each interval to total well influx, is determined. Therefore, it is possible to estimate the production profile of a well from the correlations established between the petrophysical properties and %APP.

CONCLUSIONS

The methodology developed in this study demonstrates a clear relation between rock types and flow rates in the study area. Normalized petrophysical and production parameters that can be easily correlated were generated. The upscaling process eliminated the variables that affect flow behavior, and allowed the definition of production contribution as a function of the petrophysical properties of the producing intervals.

Ranking flow units according to their K/PHI ratio is extremely helpful for understanding the flow behavior of a reservoir, since this ratio is entailed to the flow potential of the different flow units.

Fluid properties have an important influence in the petrophysics-production relation. In oil producing wells, the percentage of flow contribution resulted more dependent on rock quality, than in gas/condensate producing wells, showing a linear relationship.

With the correct determination of the petrophysical properties of a perforated interval, and the knowledge of the fluid properties, it is possible to estimate production in the study area.

NOMENCLATURE

APP = flow contribution per foot
FUSM = relation between %K/H and %PHI/H, *%*
H = thickness, *ft*
k_{air} = uncorrected air permeability, *md*
K*H = flow capacity
PF = rock type curve
PHI*H = storage capacity
ϕ = total core porosity, *%*
ϕ_e = effective porosity, *fraction*
Q = flow rate, *bbl/day*
%Q = percentage of total flow rate for a given interval
RPS = revolutions per second
R35 = pore aperture radius (35^{th} percentile), μ
R45 = pore aperture radius (45^{th} percentile), μ

REFERENCES

Gunter, G.W., Finneran, J.M., Hartmann, D.J. and Miller J.D., Early Determination of Reservoir Flow Units Using an Integrated Petrophysical Method, SPE 38679, Annual Technical Conference and Exhibition, pp. 373-380.

Kolodzie, S., Jr., Analysis of Pore Throat Size and Use of the Waxman-Smits Equation to determine OOIP in Spindle Field, Colorado: Society of Petroleum Engineers, 55th Annual Fall Technology Conference, Paper SPE 9382, (1980) 10 pp.

León, H., Técnicas de Perfilaje de Producción en Maracaibo (1968), v. III, pp. 1-8.

Pittman, E. D., Relationship of Porosity and Permeability to Various Parameters Derived from Mercury Injection Capillary Pressure Curves for Sandstone: AAPG Bulletin, (1992) v. 76, No. 2, pp. 191 - 198.

Porras, J.C., Rock Typing: A Key Approach for Petrophysical Characterization and Definition of Flow Units, Santa Barbara Field, Eastern Venezuela Basin, VII Latin American and Caribbean Petroleum Engineering Conference, Paper SPE 69458 (2001), 6 pp.

Schlumberger-Western Atlas Login Service, Interpretative Methods for Production Well Logs, IV Edition

Winland, H. D., Oil Accumulation in Response to Pore Size Changes, Weyburn Field, Saskatchewan, (1972) Amoco Production Research Report No. F72-G-25.